Front. Earth Sci. 2022, 16(4): 949–962
https://doi.org/10.1007/s11707-022-0979-0

RESEARCH ARTICLE

Paleosalinity and lake level fluctuations of the 3rd Member of Paleogene Shahejie Formation, Chezhen Sag, Bohai Bay Basin

Long SUN[1], Jinliang ZHANG (✉)[1], Yang LI[2], Xue YAN[1], Xuecai ZHANG[3]

1 Faculty of Geographical Science, Beijing Normal University, Beijing 100875, China
2 Hubei Key Laboratory of Petroleum Geochemistry and Environment, Yangtze University, Wuhan 430100, China
3 Oil and Gas Exploration Management Center, Sinopec Shengli Oilfield, Dongying 257000, China

Abstract The Chezhen Sag, located in the north-western Jiyang Depression, is one of the most important oil-bearing sags in the Bohai Bay Basin. Due to the low degree of exploration in the sag, paleosalinity and sedimentary environment of the sag in the 3rd Member of Paleogene Shahejie Formation (Es3) is not clear. Recovering the paleosalinity and lake level fluctuations is helpful for understanding organic matter rich rocks sedimentation. Therefore, a detailed geochemical, mineralogical and paleontological analysis of the Es3 in the Chezhen Sag was conducted. Index like Sr/Ba ratios, B/Ga ratios, equivalent boron content and methods concluding Adams' formula and Couch's method were adopted to reveal the paleosalinity and lake level variations. The results indicate that the lower submember (Lower Es3) was deposited in a salt water with high salinity, accompanied by dry climate and transgression event. The middle submember (Middle Es3) and upper submember (Upper Es3) record a freshwater to brackish environment. The paleosalinity and paleoclimate changes are consistent with the global sea level variations. The type and content of sporopollen indicate a dry climate in Lower Es3, which further confirms the reliability of the reconstruction results of paleosalinity. Combined with the paleoclimate and previous marine paleontological evidence, we proposed that the high salinity period is associated with a high lake level and a large-scale transgression event in Lower Es3. According to salinities and corresponding Lake depths, we established a sedimentary environment variation model of the Es3 Member in Chezhen Sag.

Keywords Chezhen Sag, paleosalinity, paleoclimate, boron lake level

Received September 16, 2021; accepted February 17, 2022

E-mail: jinliang@bnu.edu.cn

1 Introduction

Paleosalinity recovery can provide evidence for identifying paleowater types, marine incursions, sedimentary facies and sedimentary environment evolution (Degens et al., 1957; Landergren, 1958; Zheng and Liu, 1999; Du et al., 2016; Zhang et al., 2017; Wei et al., 2018). The main methods for determining paleosalinity are: 1) descriptive analysis using petrology, fossils and organic geochemistry; 2) semiquantitative analysis using elemental geochemical test data like Sr/Ba ratios, B/Ga ratios, equivalent boron contents, and so on; and 3) quantitative analysis based on elemental geochemistry and other lithogeochemistry indicators such as Adams' formula and Couch's method (Walker and Price, 1963; Qian and Shi, 1982; Xiong and Xiao, 2011; Zhang et al., 2016; Sun et al., 2022). In addition to the above parameters, unconventional methods such as depositing phosphate, carbon and oxygen isotopes are also widely used. (Frederickson and Reynolds, 1959; Curtis, 1964; Lerman, 1966; Seward, 1978; Rohling, 2007; Zhang et al., 2017). However, imperfect discrimination criteria and inconsistent discrimination still exists (Schmidt, 1999; Du et al., 2016).

Boron was used as an effective salinity index since 1950s (Degens et al., 1957). The boron contents of marine fine grained deposits are higher than those of continental sediments (Walker, 1968; Harder, 1970; Furst, 1981; Legler et al., 2011). Since then, a series of paleosalinity reconstruction methods based on boron content have been established, such as equivalent boron content, Adams' formula and Couch's method (Walker and Price, 1963; Adams et al., 1965; Walker, 1968; Couch, 1971). In addition, sedimentologists also pointed out that the B/Ga and Sr/Ba ratios are unequal in various depositional environments (Qian and Shi, 1982; Zheng and Liu, 1999, Xiong and Xiao, 2011). As the seawater salinity increases

from continental to marine environments, increasing amounts of strontium (Sr) will precipitate as $SrSO_4$ (Wang et al., 1979). By calculating the Sr/Ba ratios, the types of water bodies and paleosalinities can be indirectly distinguished. In some studies, the Sr/Ba ratios were below 0.6 for freshwater, 0.6–1 for brackish water and above 1 for seawater (Qian and Shi, 1982). From continental to marine environments, gallium (Ga) decreases with sediment deposition, whereas boron can migrate far offshore, so the B/Ga ratios can reflect the depositional environments (Potter et al., 1963; Shimp et al., 1969; Yuri et al., 2008). The B/Ga ratios are below 3 for freshwater, 3–4.5 for brackish water, and above 4.5 for salty water (Wang and Wu, 1983).

The 3rd Member of the Shahejie Formation (Es3), which was deposited in the Middle Eocene of the Paleogene, is one of the most promising oil-producing section in the Chezhen Sag, with a high potential for shale oil development. At present, the paleosalinities and their variations in specific stages have not been studied in depth, and there are disputes regarding the sedimentary environments and characteristics of the palaeowater bodies in the subsegments of the sag. It is considered that the high paleosalinity and hydrocarbon generation potential in Lower Es3 submember may be related to possible marine incursions (Wei et al., 2018). However, to date, the time and scope of transgression and the preservation of high-quality source rocks have not been systematically discussed. It is of great significance to study the transgression events and deposition of high-quality source rocks (Ma et al., 2016).

Taking the Es3 Member of the Paleogene in Chezhen Sag as an example, this study mainly uses the elemental geochemical method, including Sr/Ba ratios, B/Ga ratios, equivalent boron contents, Adams' formula and Couch's method to determine and analyze the salinity during the sedimentary period of the Es3 Member. The co-evolution of paleosalinity and paleoclimate is discussed, and the relationship between paleosalinities, lake level fluctuations and global sea level changes is analyzed.

2 Geological setting

The Chezhen Sag is located in the northern Jiyang Depression in the Bohai Bay Basin (Li et al., 2021). It is a typical dustpan-shaped fault basin with the structural characteristics of a northern fault and overspread south (Lao et al., 2019; Li et al., 2022). From north to south, the Chezhen Sag can be divided into three sub tectonic units: a northern steep slope zone, central sag zone and southern gentle slope zone. From west to east, the Chezhen Sag can be divided into the Chexi subsag, Dawangbei subsag and Guojuzi subsag (Figs. 1(a) and 1(b)). The drilled strata are mainly located in the Palaeocene Shahejie Formation (Es), which contains a large set of sandy gravels, mudstones and small amounts of gypsum deposits. The Es is divided from bottom to top into four members: Es4, Es3, Es2, and Es1. The Es3 Member of the studied formation is further subdivided from bottom to top into three submembers including Lower Es3, Middle Es3, and Upper Es3 (Fig. 1(c)).

The Es3 Member was deposited during a period of intense faulting activity, and multitype and multistage conglomerate bodies were widely developed. Therefore, the relevant research on the Chezhen Sag has focused on the sand and conglomerate distributions, classifications of depositional stages, reservoir properties and reservoir formation mechanisms. It is believed that Es3 Member in the Chezhen Sag is dominated by shallow lacustrine and semi-deep lacustrine facies, with small fan deltas and turbidite fans that mainly developed in the Upper Es3 and Middle Es3 and nearshore submarine fans and sublacustrine fans that mainly developed in the Lower Es3. However, the specific characteristics of the palaeowater bodies, which are mainly analyzed by using paleontological trace fossils, are not known (Shi et al., 2004). Relatively few studies have used geochemical methods to recover salinities of palaeowater bodies. To clarify the salinity backgrounds of palaeowater bodies, the paleosalinity characteristics, paleoclimate and lake level fluctuations of the Es3 Member in the Chezhen Sag are studied in this paper.

3 Materials and methods

3.1 Samples and experiments

The study area is divided from west to east into three subsags: the Chexi subsag, Dawangbei subsag and Guojuzi subsag. From north to south, it is divided into three sub tectonic units: a northern steep slope zone, central depression zone and southern gentle slope zone. In this study, 9 samples from 5 wells (e.g., wells C40, C663, D651, D92, and G1) were collected (Fig. 1(a), Table 1). To ensure the accuracy and rationality of the results, 1–2 core wells from each subsag are selected for sampling, and the distribution of samples covers different subsags and secondary tectonic units (Fig. 1(a)). The main lithology of the samples consists of mudstone and siltstone. Among the samples there are 4 samples from Lower Es3, 2 samples from Middle Es3 and 3 samples from Upper Es3 (Table 1).

Detrital boron that disturbs paleosalinity reconstructions is mainly derived from tourmaline, a type of heavy boron-rich mineral in the coarser fraction of the sediments (normally >5 μm) (Walker and Price, 1963; Ye et al., 2016). To reconstruct the paleosalinity and paleoenvironment more accurately, the <5 μm fraction of samples was

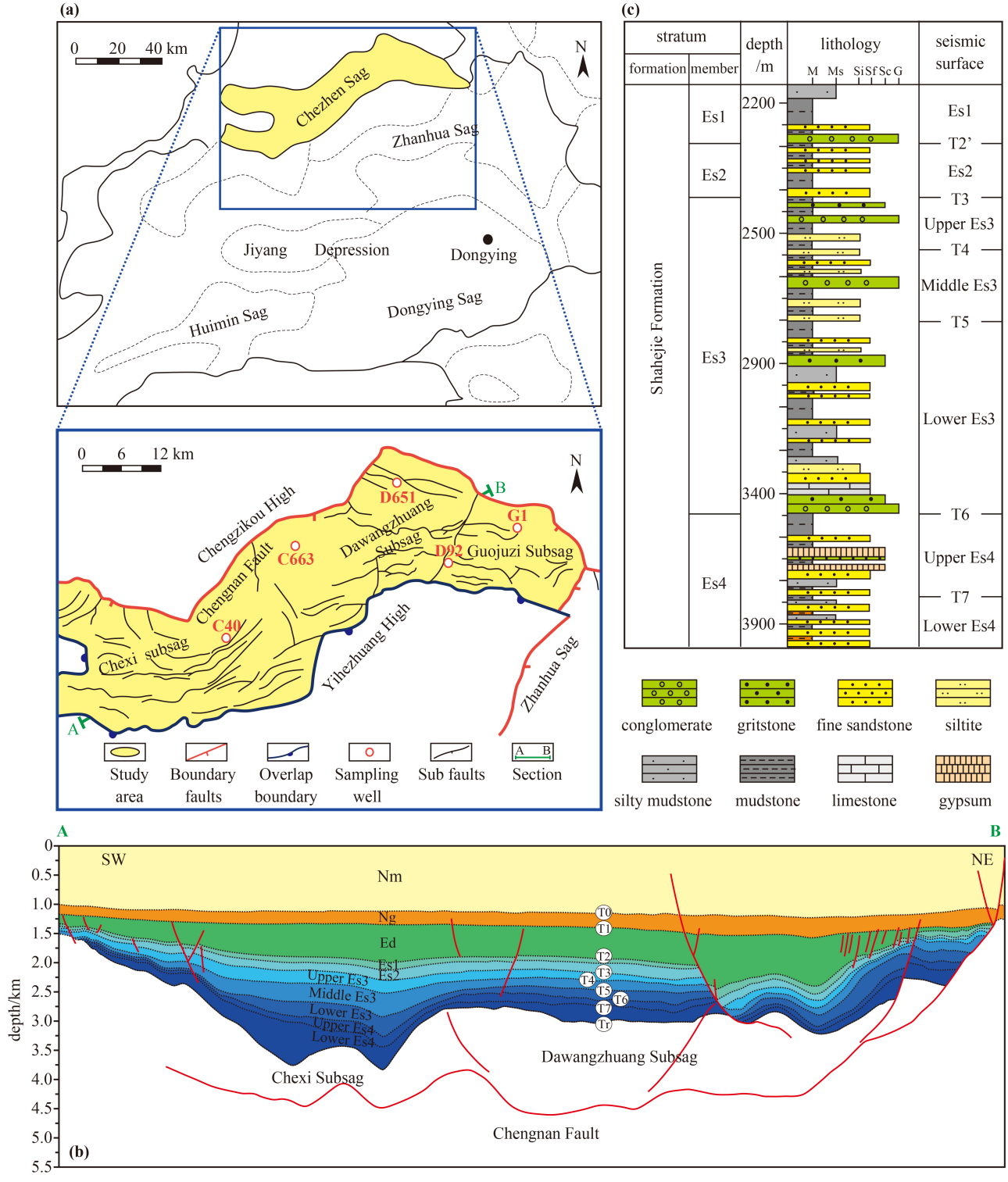

Fig. 1 Location (a), main structural units (b) and stratigraphic units (c) of the Chezhen Sag. (a) Structural location of the Chezhen Sag in the Bohai Bay Basin and its main structural sub tectonic units. (b) 2D seismic section at Line A−B. Geological surfaces of the seismic reflections: T0-boundary between the Minghuazhen Formation (Nm) and Guantao Formation (Ng); T1-boundary between the Guantao Formation (Ng) and Dongying Formation (Ed), which is also the surface between the Palaeocene and Eocene; T2-boundary between the Dongying Formation (Ed) and Shahejie Formation (Es); T3-surface between Es2 and Upper Es3; T4-surface between Upper Es3 and Middle Es3; T5-surface between Middle Es3 and Lower Es3; T6-surface between Lower Es3 and Upper Es4; T7-surface between Upper Es4 and Lower Es4; Tr-boundary between the Shahejie Formation (Es) and Majiagou Formation (Om), which is also the surface between the Paleogene and Ordovician. (c) The main stratigraphic units of the Shahejie Formation in the Chezhen Sag.

Table 1 Samples and content test results for selected elements in the study area

Well	Sample	Depth/m	Member	Lithology	B/‰	Sr/‰	Ba/‰	Ga/‰	K_2O/%
D651	D651-1	2387.4	Upper Es3	siltstone	97.9	288	525	24.5	3.29
C40	C40-1	2632.0	Upper Es3	mudstone	80.8	420	460	21.8	2.93
C40	C40-2	2653.5	Upper Es3	mudstone	96.3	370	453	24.2	3.16
C40	C40-3	2841.9	Middle Es3	mudstone	54.0	291	421	21.2	2.22
C40	C40-4	2855.1	Middle Es3	mudstone	43.6	313	425	19.2	2.00
G1	G1-1	3611.2	Lower Es3	mudstone	69.9	397	407	15.6	1.98
G1	G1-2	4101.2	Lower Es3	mudstone	69.2	678	397	14.5	1.37
D92	D92-1	2625.3	Lower Es3	siltstone	63.7	850	487	14.4	2.51
C663	C663-1	3883.0	Lower Es3	mudstone	69.8	610	267	12.2	1.52

Notes: B-boron, Sr-strontium, Ba-barium, Ga-gallium, K_2O-potassium oxide.

further dried (Ye et al., 2016; Zhang et al., 2017) and ground into a powder for elemental analyses at the Institute of Sinopec Shengli Oilfield Exploration and Development Research, Dongying. A mixture of HF and HNO_3 was used to digest approximately 20 mg of each sample in a Teflon container by using pressurized acid digestion. After the experimental treatment described above, nine samples were analyzed to determine their trace element (e.g., B, Sr, Ba, and Ga) and major element (e.g., K_2O) concentrations using an inductively coupled plasma atomic emission spectrometry (ICP-AES) system that was manufactured by Agilent VISTA (Table 1). The relative standard deviations of the elements were less than 5%, as determined by replicate analyses.

Similarly, the clay fractions <5 μm were collected by gravitational division according to Stokes' law (Ye et al., 2016; Zhang et al., 2017). The samples were then analyzed for their clay mineral contents by XRD with a D/max-2500pc diffractometer in accordance with "SYT 5163-2010" (Biscaye, 1965; Zeng et al., 2010; Li et al., 2019) (Table 2). The test procedure and analytical results were sufficiently reliable, and the relative errors of the analytical results for all test samples in this study were less than 5%.

Sporopollen identification was carried out in the Stratigraphy Research Room of the Shengli Oilfield Exploration and Development Research, Dongying. For sporopollen analysis, approximately 5 g of sample from well C40 was weighed and dried. To remove humic acid from the sample, a mixture of potassium chlorate and nitric acid was used for decomposition and oxidation. To wash the sample to neutral pH, sodium carbonate with pH concentration of 1% was added to the sample and heated to boiling (>1 h). Then the aperture is 10 μm sieve was used to enrich sporopollen and glycerol was added to obtain thin section containing sporopollen. The main types and contents of sporopollen were identified by binocular biomicroscope (Table 4).

3.2 Paleosalinity reconstruction method

The boron contents of argillaceous sediments have a

Table 2 Relative contents (%) of the minerals analyzed by X-ray diffraction in the study area

Number	Sample	Depth/m	Member	Test content/%					Mixed-layer/%
				S	I + S	I	K	Ch	I/S in I + S
1	C40-1	2632.0	Upper Es3	0	49	42	5	4	11
2	C40-2	2653.5	Upper Es3	0	53	43	4	0	8
3	C40-3	2841.9	Middle Es3	0	64	33	3	0	19
4	C40-4	2855.1	Middle Es3	0	47	36	17	0	16
5	G1-1	3611.2	Lower Es3	0	26	69	5	0	16
6	G1-2	4101.2	Lower Es3	0	51	44	5	0	16
7	C663-1	3883.0	Lower Es3	0	54	36	10	0	12

Notes: S-montmorillonite, I-illite, K-kaolinite, Ch-chlorite, I + S-illite and montmorillonite mixed layer, and I/S-illite content/montmorillonite content in I + S.

linear positive correlation with paleosalinity (Frederickson and Reynold, 1959). Walker and Price (1963) demonstrated that the boron in argillaceous sediment samples is predominantly present in illite. The boron and illite contents are first transformed into adjusted boron and equivalent boron, which are related to paleontology (Fig. 2). The average K_2O content in illite is 8.5%. It is assumed that all of the potassium (K) is derived from illite. On this basis, the boron content can be adjusted to the boron from pure illite. The adjusted boron content is calculated follows:

$$B_a = \frac{B_t \times 8.5}{K_2O}, \quad (1)$$

where B_a: adjusted boron content, ‰; B_t: tested boron content, ‰; K_2O: K_2O content, %.

The threshold values for the equivalent boron amounts in various water bodies are different. Studies have shown that the values in fresh water are below 200‰, those in brackish water range from 200‰ to 300‰ and those in salty water are greater than 300 ‰ (Walker and Price, 1963; Walker, 1968).

There is a direct correlation between the equivalent boron contents and depositional salinities of sediments (Adams et al., 1965). The relationship between the paleosalinity (Sp_a) and equivalent boron content (B_e) is as follows:

$$Sp_a = 0.0977 \times B_e - 7.043, \quad (2)$$

where Sp_a: paleosalinity calculated by Adams, ‰; B_e: equivalent boron content, ‰.

In addition to the above method, Couch (1971) calculated the palaeosalinities of kaolinitic Tertiary shales in Nigeria based on their equivalent boron contents in combination with isothermal adsorption curves (Couch, 1971). The calculation formula for the paleosalinity is recalibrated:

$$B_k = \frac{B_t}{4X_i + 2X_m + X_k} X_k, \quad (3)$$

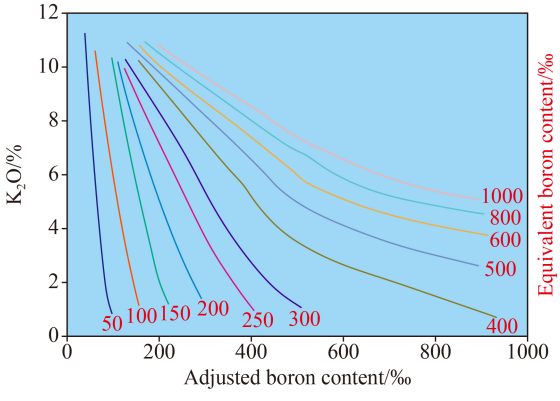

Fig. 2 Equivalent boron content curve (Modified after Walker and Price, 1963).

where B_t: tested boron content, ‰; X_i: relative content of illite, %; X_m: relative content of montmorillonite, %; X_k: relative content of kaolinite, %.

$$\lg Sp_c = \frac{\lg B_k - 0.11}{1.28}, \quad (4)$$

where Sp_c: paleosalinity calculated by Couch, ‰; B_k: boron content of kaolinite, ‰.

When comparing the above two methods, Couch's method considers the adsorption capacities of different clay minerals, not only illite. This method has a wider range of application and higher reliability than Adams' formula.

4 Results

4.1 Results of Sr/Ba and B/Ga ratios

The Sr/Ba ratios determined from wells, such as well D651 in the Chezhen Sag, were calculated based on the Sr/Ba ratio method (Table 3). By using the corresponding relationship between the Sr/Ba ratio and paleosalinity, the elemental ratios of the Es3 Member in the Chezhen Sag were plotted (Fig. 3(a)). The results show that the average Sr/Ba ratio of the Es3 Member in the study area is 1.16, which generally indicates a mixed water of brackish and salt water. The average Sr/Ba ratio for Lower Es3 is 1.68, with the highest value of 2.28 and lowest value of 0.98. The average Sr/Ba ratio for Middle Es3 is 0.71, with the highest value of 0.74 and lowest value of 0.69. The average Sr/Ba ratio for Upper Es3 is 0.76, with the highest value of 0.91 and lowest value of 0.55. The salinity of the Lower Es3 submember is the highest. The water bodies gradually changed from salt water to brackish water. In summary, from an overall view provided by the Sr/Ba ratio method, the Es3 Member in the study area was located in a mixed water environment of brackish and salt water, and the salinity gradually decreased from Lower Es3 to Upper Es3.

The B/Ga ratios of the Es3 Member in the study area vary significantly, with a mean value of 3.99, and generally indicate a brackish water environment (Fig. 3(b)). The results show that the mean value of the B/Ga ratios in Lower Es3 is 4.85, with the highest value of 5.72 and lowest value of 4.42, which indicates a salty water environment. The mean value of the B/Ga ratios in Middle Es3 is 2.41, with a maximum value of 2.55 and minimum value of 2.27, which indicates a freshwater environment. The mean value of the B/Ga ratios in Upper Es3 in the study area is 3.89, with a maximum value of 4 and minimum value of 3.71, which indicates an overall brackish water environment. According to the B/Ga ratio method, there is a wide range of B/Ga ratios, and the paleosalinity that corresponds to the Es3 Member in the

Table 3 Results of the paleosalinity analyses for the study area

Sample	Member	Sr/Ba	B/Ga	B_a/‰	B_e/‰	Sp_a/‰	Sp_c/‰
D651-1	Upper Es3	0.55	4	252.93	206.30	13.11	/
C40-1	Upper Es3	0.91	3.71	234.40	183.43	10.88	11.32
C40-2	Upper Es3	0.82	3.98	259.03	208.10	13.29	12.67
C40-3	Middle Es3	0.69	2.55	206.76	149.81	7.59	8.2
C40-4	Middle Es3	0.74	2.27	185.30	131.24	5.78	7.25
G1-1	Lower Es3	0.98	4.48	236.71	176.86	10.24	8.7
G1-2	Lower Es3	1.71	4.77	297.07	209.98	13.47	9.6
D92-1	Lower Es3	1.75	4.42	395.22	268.02	18.65	/
C663-1	Lower Es3	2.28	5.72	390.33	269.55	18.71	10.31

Notes: Sr/Ba-ratio of strontium to barium, B/Ga-ratio of boron to gallium, B_a-adjusted boron content, B_e-equivalent boron content, Sp_a-paleosalinity calculated by Adams' method, Sp_c-paleosalinity calculated by Couch's method.

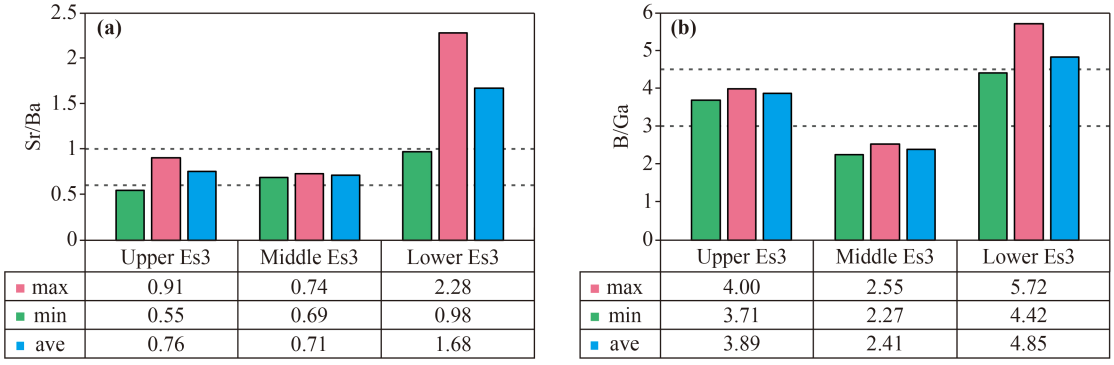

Fig. 3 Sr/Ba and B/Ga ratios of nine samples from the study area.

study area indicates a mixed water environment of fresh and salt water.

It is clear that the values of the Sr/Ba and B/Ga ratios can only be used as qualitative indicators for the paleosalinity of water body (Zhang et al., 2017), and other indicators or methods, such as the equivalent boron contents and quantitative calculations, are needed for quantitative studies of the paleosalinity.

4.2 Results of the equivalent boron contents

Based on the tested elemental contents (Table 1), the equivalent boron contents of the Es3 Member in the study area were calculated (Fig. 4). The data show that the average value of the equivalent boron content in the Es3 Member is 200.37‰. The equivalent boron content in Lower Es3 is the highest, with an average value of 231.1‰, while that in Middle Es3 is the lowest, with an average value of 140.53‰. The salinities first decreased and then increased gradually from Lower Es3 to Upper Es3. In general, the Es3 Member in the Chezhen Sag was deposited in a slightly brackish water environment. This result is generally consistent with the conclusions obtained from the above Sr/Ba and B/Ga ratio methods.

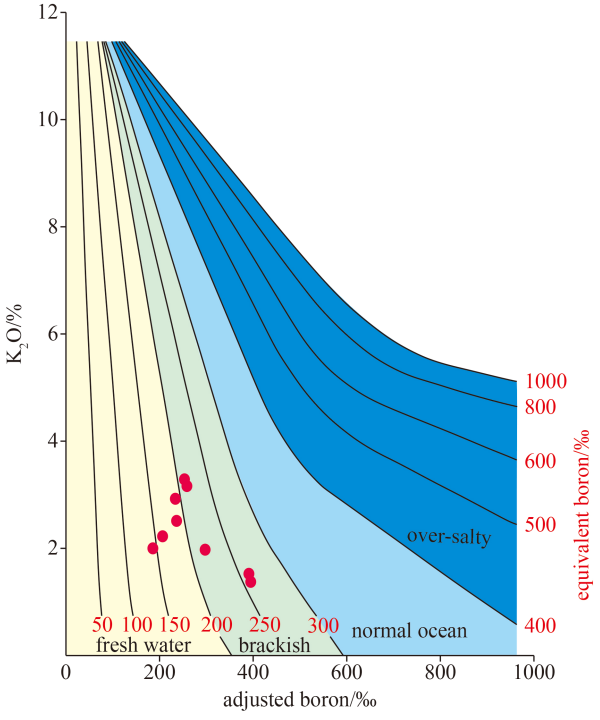

Fig. 4 Equivalent boron content distribution in the study area.

4.3 Results of quantitative calculations of paleosalinity

The paleosalinity values from Adams' formula (Sp_a) are calculated from the equivalent boron contents (Table 3). The paleosalinities of the Es3 Member in the Chezhen Sag range between 5.78‰ and 18.71‰, and the average value is 12.41‰. According to the salinity grade of the water body (Walker, 1968), Adams' method indicates a brackish to salty water environment.

Based on the correspondence between paleosalinities and water body types, the boron contents (Table 1) and clay mineral contents (Table 3, Fig. 5) were used to calculate the paleosalinity values by using Couch's method (Sp_c). By using this method, the average paleosalinity of the Es3 Member was 9.72‰, with a maximum value of 12.67‰ and minimum value of 7.25‰ (Table 3), which indicates brackish water. The results are consistent with those obtained by the above methods and reflect the salinity characteristics of the entire water body. The evolution trend of the salinities that were obtained by various methods is consistent, which first decreases and then increases (Wei et al., 2018).

5 Discussion

5.1 Paleoclimate and paleosalinity co-evolution

Numerous studies have shown that the pollen and ostracod species in modern settings are sensitive to various environmental parameters, including salinity, and are therefore widely employed to infer the salinities and climate changes in sediments (De Deckker et al., 1988; Frenzel and Boomer, 2005; Ye et al., 2016). Various plants have different degrees of success under different climatic conditions, and thus, sporopollen fossils can reflect the type of climate during a depositional period. Based on the sporopollen obtained from the Es3 Member in well C40, the paleoclimatic characteristics of the Es3 Member in the Chezhen Sag are initially determined. After analyzing 1990 sporopollen fossils from the Es3 Member in well C40, a total of 59 species of sporopollen fossils were identified. The main sporopollen fossils in the study area are *Quercoites*, *Ulmipollenites*, *Abietineae pollenites* and *Ephedripites*. According to the absolute contents of the main sporopollen fossils (Fig. 6, Table 4) and the percentage contents of the main sporopollen fossils (Fig. 7), the main types of sporopollen fossils in the Es3 Member in well C40 are angiosperms, which account for 70.25% of all sporopollen fossils, gymnosperms for 28.69% of all sporopollen fossils, and pteridophytes for only 0.80%. By using the variations in sporopollen fossil contents, the Es3 Member in well C40 can be divided into two sporopollen zones (e.g., H1 and H2) (Fig. 6).

Based on the calculations of the percentages of the main sporopollen fossils in the Es3 Member in well C40, it is considered that the climate during deposition of the Es3 Member in the study area had the characteristics of periodicity and cyclicity. The relatively flourishing sporopollen assemblage consisting of *Quercoites*, *Ulmipollenites*, *Abietineaepollenites*, and *Ephedripites* indicates that the climate of the sedimentary period consisted of a relatively dry subtropical climate. The

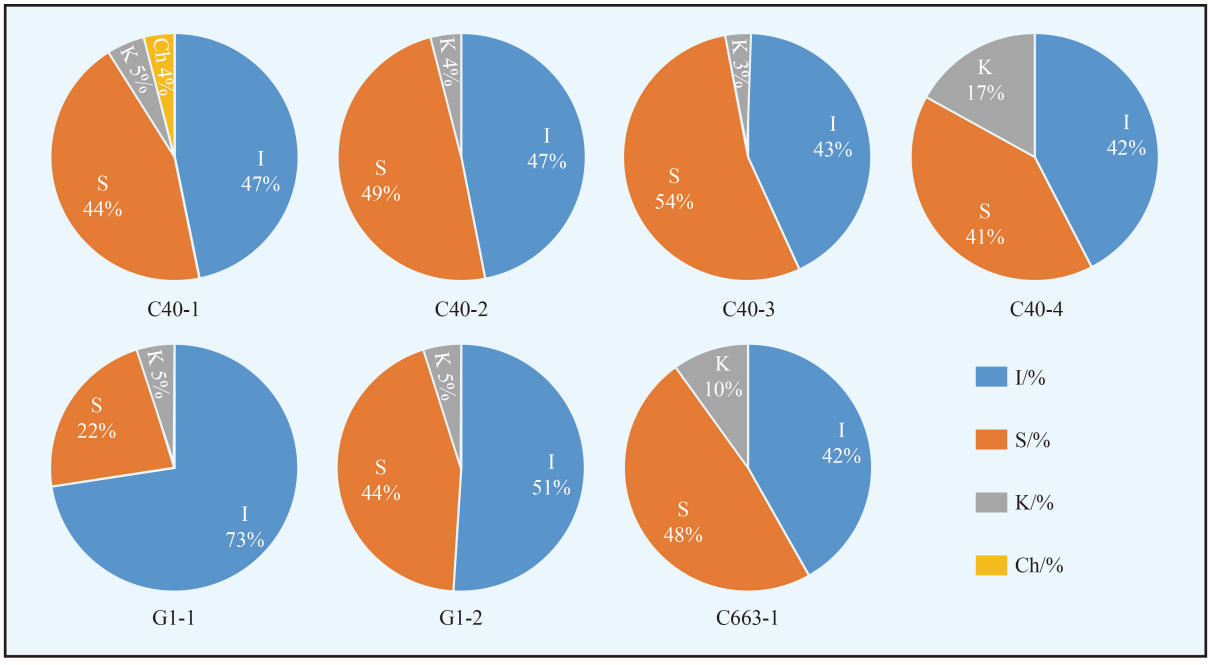

Fig. 5 XRD analyses of seven representative samples. S-montmorillonite, I-illite, K-kaolinite, and Ch-chlorite.

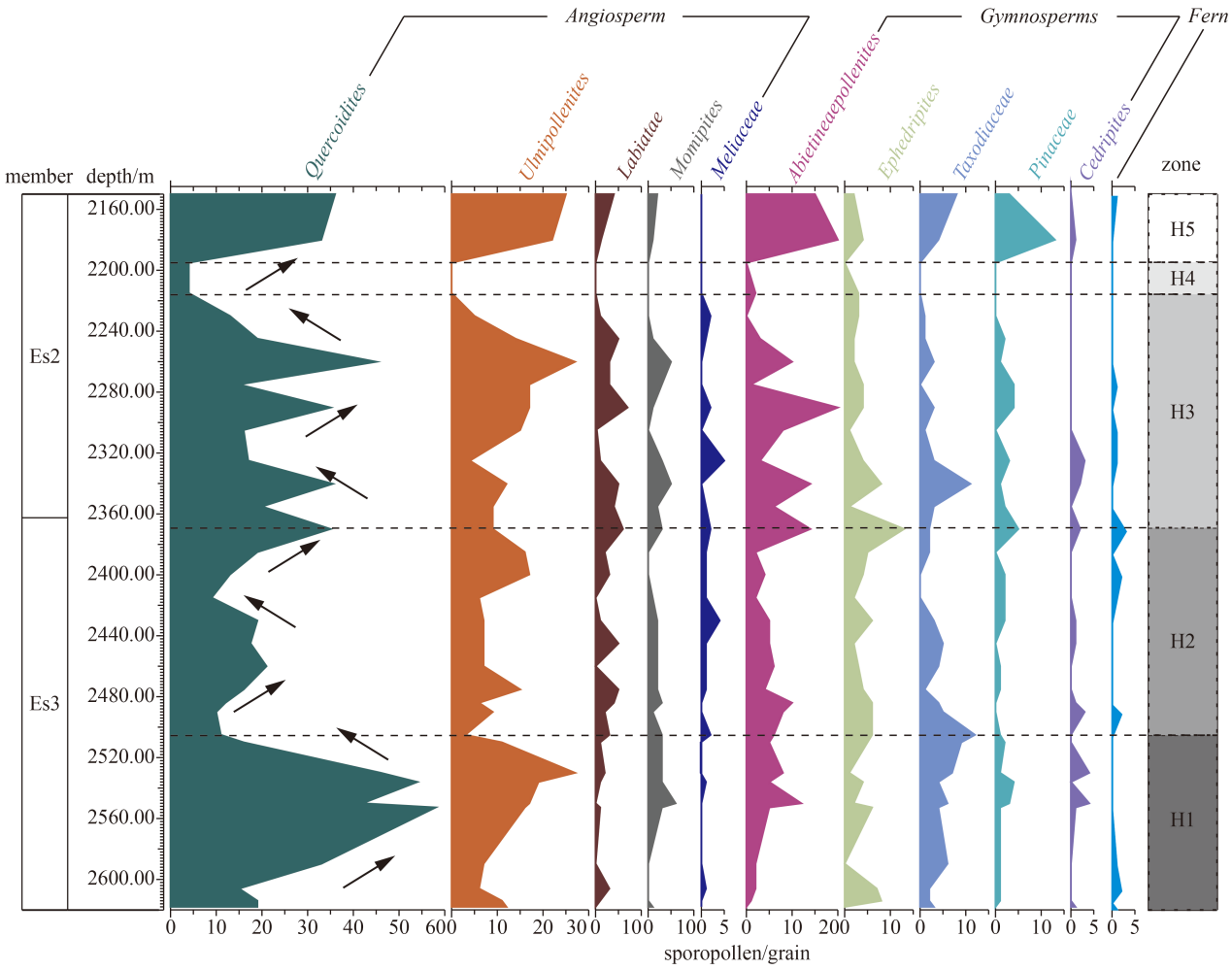

Fig. 6 Absolute contents of the main sporopollen fossils in the study area.

relative contents of the main sporopollen fossils in the Es3 Member of well C40 show that *Quercoidites*, *Ulmipollenites*, *Abietineaepollenites*, and *Ephedripites* have negative correlations between the climate types that are indicated by the index. As a result, the climate of the Es3 Member in the study area evolved from dry to humid to dry (Fig. 8). Comparing the paleosalinity variations in the Es3 Member in the study area (Fig. 4) shows that the variations in paleoclimate and paleosalinity are consistent. A dry climate always corresponds to high salinity, and a humid climate often corresponds to low salinity. The accuracy of the paleosalinity reconstruction is further validated by the sporopollen-based palaeoclimatic features.

5.2 Paleosalinities and lake level fluctuations

The overall salinity of the Es3 Member in the study area is brackish, with higher initial salinity until salty water. The paleoclimate that is identified by the sporopollen is an overall dry climate, and the degree of aridity was closely related to the salinity of the water column. The salinities are higher in dry climates but lower in humid climates.

The paleosalinity evolution of the Lower Es3 submember in the Chezhen Sag of the Bohai Bay Basin shows that all paleosalinity indices gradually decreased. The decreasing paleosalinity of this sedimentary interval may record the beginning to end stage of a transgression event, which should have occurred during the deposition of the Lower Es3 submember (Fig. 8). This transgression event corresponds to the global high sea level of the Eocene and the highest growth rate of oceanic crust (Haq et al.,1987; Miller et al., 2005), which reveals the coupling of transgression events and tectonic sea level control mechanisms. In coastal sedimentary environments, the enrichments in organic matter are not necessarily proportional to the intensities of transgression events, and the brackish water sedimentary environment may have been more conducive to the development of high-quality source rocks.

Vertically, the paleosalinities exhibit a downwards

Table 4 Absolute contents (grain) of several representative sporopollen in the study area

Samples	Depth/m	*Que.*	*Ulm.*	*Laboratory.*	*Mom.*	*Mel.*	*Abi.*	*Eph.*	*Tax.*	*Pin.*	*Ced.*	*Fer.*
C40-1	2150	36	25	4	2		15	2	8	3		1
C40-2	2180	33	22	1	1		20	4	4	13	1	
C40-3	2195	4										
C40-4	2215	4					2	3				
C40-5	2230	13	5	1		2		3	1			
C40-6	2245	19	14	5	1	1	3	2	1	2		
C40-7	2260	45	27	3	5		10	2	3	1		
C40-8	2275	15	17	3	3		1	4		4		1
C40-9	2290	35	17	7	1	2	20	4	3	4		
C40-10	2305	16	15				8	1	1			1
C40-11	2325	17	4	1	3	5	3	4	3	3	3	1
C40-12	2340	36	12	5	5		14	8	11	1	2	
C40-13	2355	20	9	4	2	1	6	1	3	2		
C40-14	2370	35	9	6	3	2	14	13	2	5	2	3
C40-15	2385	19	16	2		1	2	5	2			
C40-16	2400	13	17	3		1	4	4		2		2
C40-17	2415	9	6		1	1	2	2		2		1
C40-18	2430	19	7	1	2	4	5	6	3	2	1	
C40-19	2445	18	7	5	2	1	5	2	5		1	
C40-20	2460	21	7		2	1	6	3	4	1		
C40-21	2475	16	15	5	2	1	4	4	1	1		
C40-22	2484	12	6	4	3		10	6	4		1	
C40-23	2490	10	9	2	1		8	6	5		3	2
C40-24	2505	11	3	3	3	2	6	6	12	1		
C40-25	2510	16	11	1	1		5	5	9	2		
C40-26	2530	46	27	2	3		8	1	7	1	4	
C40-27	2536	54	19	1	3	1	5	4	4	4		
C40-28	2550	42	17		6		12	2	6	3	4	
C40-29	2552	58	16	1	3		5	6	4	1	1	
C40-30	2590	33	7				2		6	1		1
C40-31	2606	15	6	3		1	2	7	2	1		2
C40-32	2614	19	11	1			1	8	2	1		
C40-33	2618	19	12		1				3		1	1

Notes: *Que.* = *Quercoidites*, *Ulm.* = *Ulmipollenites*, *Laboratory.* = *Labiatae*, *Mom.* = *Momipites*, *Mel.* = *Meliaceae*, *Abi.* = *Abietineaepollenites*, *Eph.* = *Ephedripites*, *Tax.* = *Taxodiaceae*, *Pin.* = *Pinaceae*, *Ced.* = *Cedripites*, *Fer.* = *Fern*.

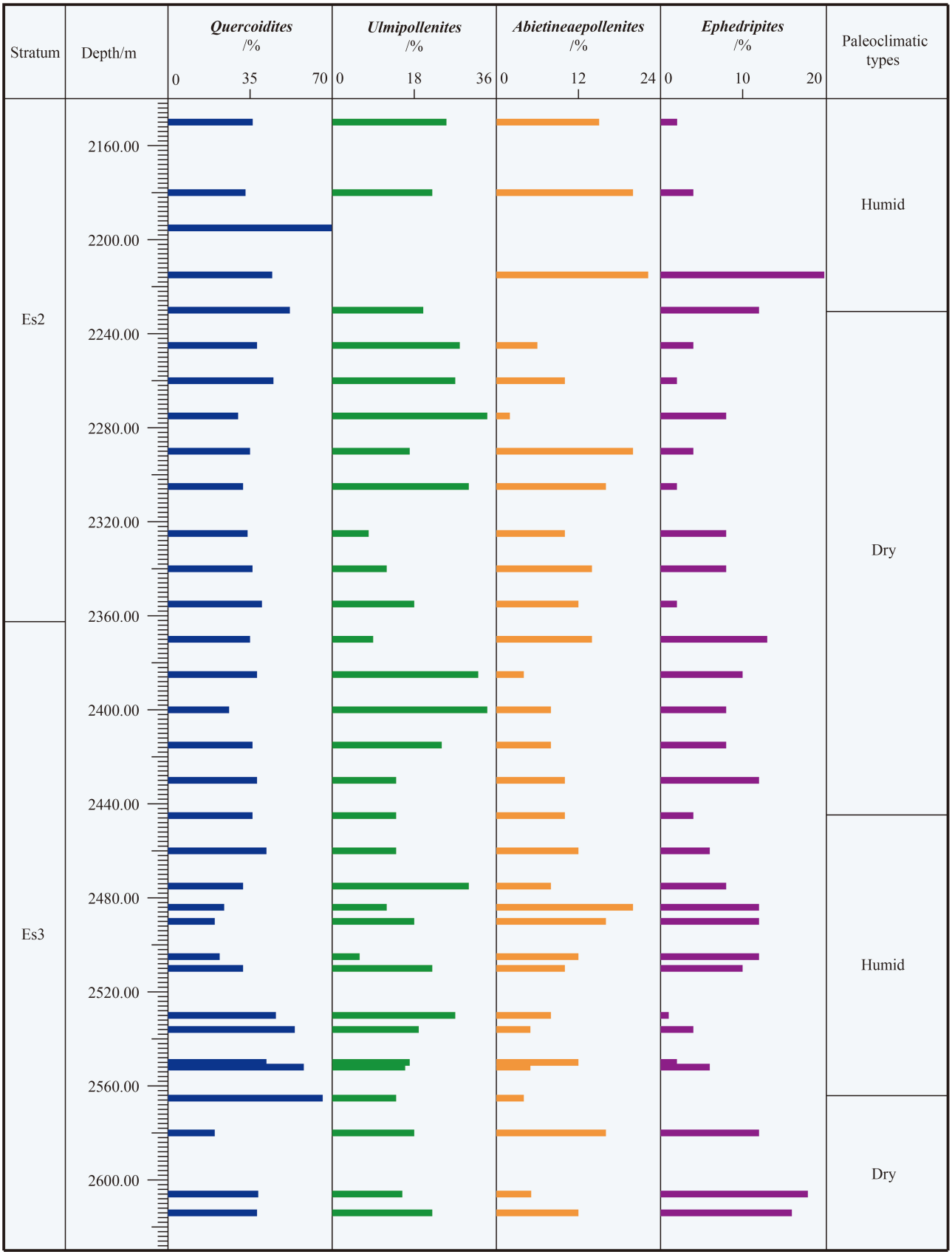

Fig. 7 Relative contents of the main sporopollen fossils and paleoclimatic types in the study area.

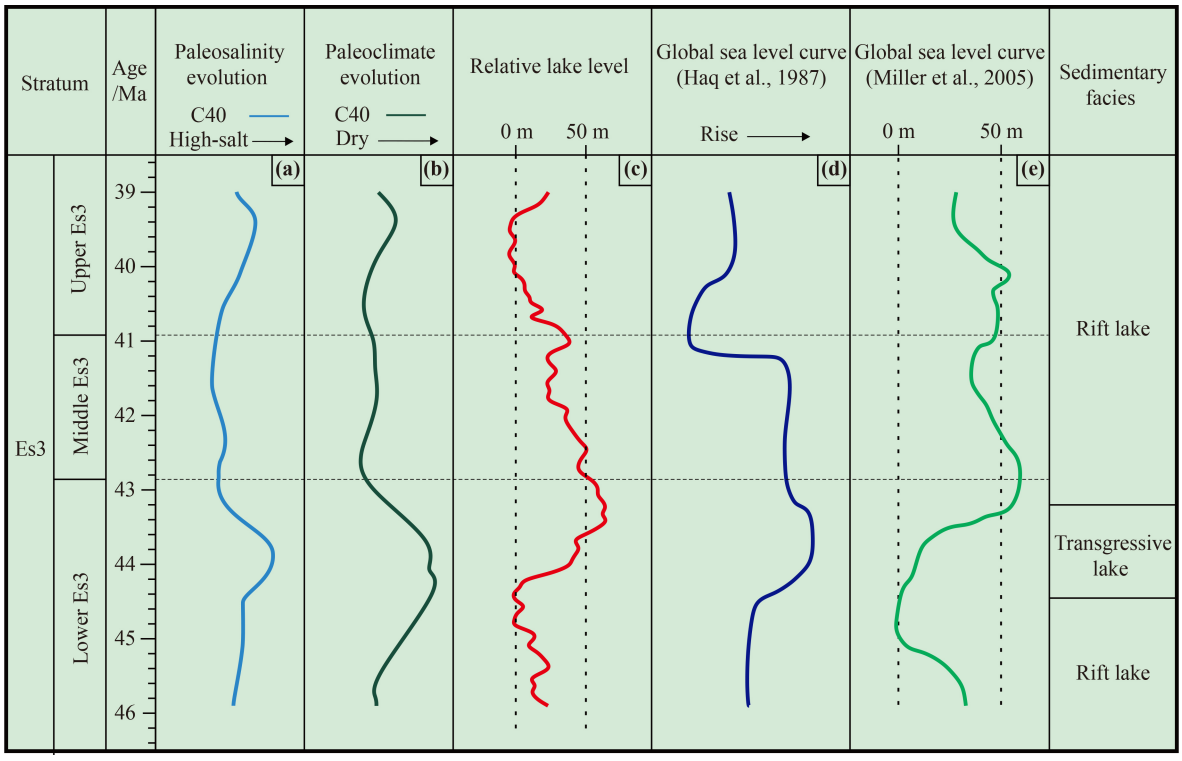

Fig. 8 Paleosalinity, paleoclimate and relative lake level changes in the study area.

trend from the Lower Es3 to Upper Es3 stages (Figs. 3 and 8). The lake water salinities in open lakes are generally controlled by transgressive events and are regarded as sensitive indicators of relative lake level changes (Ye et al., 2016). The evidence of marine paleontology indicates the existence of transgressive events in the bottom of Es3 (Wei et al., 2018). As transgression occurs, the salinities of lake water bodies gradually increase, as do the water depths (Li and Pang, 2004). Debris flow fans, terminal fans and other fans enter the water and become underwater fan deltas (Fig. 9(c)). In contrast, with the regression event, the lake water salinity decreased, the water depths became shallower, and the fan bodies were exposed underwater (Figs. 9(a) and 9(b)). Therefore, the variations in the sedimentary environment are related to the changes in paleosalinities and lake levels.

6 Conclusions

1) Sr/Ba ratio, which is a very sensitive index for paleosalinity reconstruction, is 0.55—2.28, indicating the mixed water characteristics of fresh and salt water. Similarly, the B/Ga ratio is between 3.71 and 5.72, showing that the salinity of paleowater body is consistent with the Sr/Ba ratio. The average value of equivalent boron content calculated by Walker's method is 200.37‰.

2) The paleosalinity values of the Es3 Member in the Chezhen Sag calculated by Adams' formula range from 5.8‰ to 18.7‰, averaging 12.4‰. The average paleosalinity calculated by Couch's method is 9.72‰, with a maximum value of 12.67 ‰ and minimum value of 7.25‰. Both Adams and Couch's methods indicate that the overall paleosalinity of the Es3 Member is mixed water of fresh and salt water. For each submember, ratios of Sr/Ba and B/Ga, Adams' formula and Couch's method all show that the salinity of Lower Es3 is the highest, Upper Es3 is the second, and Middle Es3 is the lowest.

3) Previous marine paleontological evidence indicates the existence of transgressive events in Lower Es3, which explains the reconstruction results of high salinity. The type and content of sporopollen indicate that there is a dry climate at the bottom of the Es3 Member, which further confirms the reliability of the reconstruction results of paleosalinity.

4) High salinity periods are associated with high lake levels. The increase in paleosalinity correlated with a large-scale transgression event at Lower Es3 submember. A sedimentary environment variation model of the Es3 Member in Chezhen Sag is established based on salinities and corresponding lake depths.

Acknowledgments This study was supported by the Sinopec Shengli Oilfield Cooperation Project named "Reunderstanding the sedimentary system of the third to the fourth member of the Shahejie Formation in the Chezhen Depression and the distribution of hidden traps" and China Postdoctoral Science Foundation (No. 2021M700537). We thank the Sinopec Shengli Oilfield Geological Research Institute for the drilling core samples and analytical tests. We are very grateful to the reviewers for their constructive comments and helpful suggestions, which have greatly improved the quality of this manuscript.

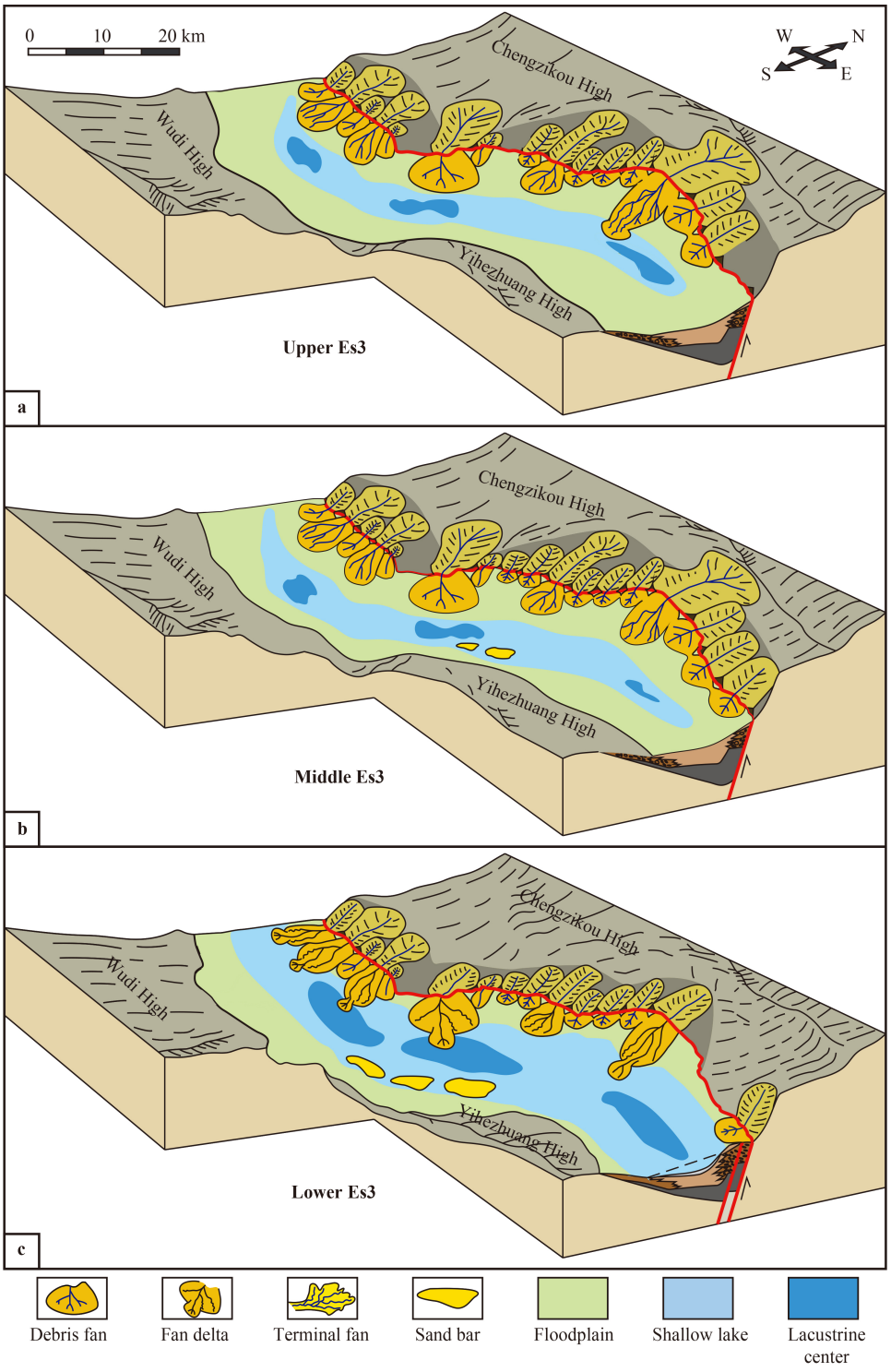

Fig. 9 Sedimentary environment variation model of the Es3 Member in the study area.

References

Adams T D, Haynes J R, Walker C T (1965). Boron in holocene illites of the Dovey estuary, Wales, and its relationship to palaeosalinity in cyclothems. Sedimentology, 4(3): 189–195

Biscaye B E (1965). Mineralogy and sedimentation of recent deep-sea clay in the Atlantic Ocean and adjacent seas and oceans. Geol Soc Am Bull, 76(7): 803–832

Couch E L (1971). Calculation of paleosalinities from boron and clay mineral data. AAPG Bull, 55: 1829–1837

Curtis C D (1964). Studies on the use of boron as a paleoenvironmental indicator. Geochim Cosmochim Acta, 28(7): 1125–1137

De Deckker P, Chivas A R, Shelley J M G, Torgersen T (1988). Ostracod shell chemistry: a new palaeoenvironmental indicator

applied to a regressive/transgressive record from the Gulf of Carpentaria, Australia. Palaeogeogr Palaeoclimatol Palaeoecol, 66(3–4): 231–241

Degens E T, Williams E G, Keith M L (1957). Environmental studies of carboniferous sediments. Part I: geochemical criteria for differentiating marine from fresh-water shales. AAPG Bull, 41: 2427–2455

Du Q X, Guo S B, Shen X L, Cao Z H, Zhang X L, Li Y S (2016). Palaeo-water characteristics of the Member 1 of Paleogene Shahejie Formation in southern Nanpu Sag, Bohai Bay Basin. J Paleogeogr, 18: 173–183 (in Chinese)

Frederickson A F, Reynolds R C (1959). Geochemical method for determining paleosalinity. Clays Clay Miner, 8(1): 203–213

Frenzel P, Boomer I (2005). The use of ostracods from marginal marine, brackish waters as bioindicators of modern and Quaternary environmental change. Palaeogeogr Palaeoclimatol Palaeoecol, 225(1–4): 68–92

Furst M J (1981). Boron in siliceous materials as a paleosalinity indicator. Geochim Cosmochim Acta, 45(1): 1–13

Haq B U, Hardenbol J, Vail P R (1987). Chronology of fluctuating sea levels since the triassic. Science, 235(4793): 1156–1167

Harder H A (1970). Boron content of sediments as a tool in facies analysis. Sediment Geol, 4(1–2): 153–175

Landergren S (1958). On the distribution of boron on different size classes in marine clay sediments. Geol Foeren Stockh Foerh, 80(1): 104–107

Lao H G, Wang Y S, Shan Y X, Hao X F, Li Q (2019). Hydrocarbon downward accumulation from an upper oil source to the oil reservoir below in an extensional basin: a case study of Chezhen Depression in the Bohai Bay Basin. Mar Pet Geol, 103: 516–525

Legler B, Schneider J W, Gebhardt U, Merten D, Gaupp R (2011). Lake deposits of moderate salinity as sensitive indicators of lake level fluctuations: example from the Upper Rotliegend saline lake (Middle–Late Permian, northeast Germany). Sediment Geol, 234(1–4): 56–69

Lerman A (1966). Boron in clays and estimation of paleosalinitys. Sedimentology, 6(4): 267–286

Li C, Zhang L K, Luo X R, Lei Y H, Yu L, Cheng M, Wang Y S, Wang Z L (2021). Overpressure generation by disequilibrium compaction or hydrocarbon generation in the Paleocene Shahejie Formation in the Chezhen Depression: insights from logging responses and basin modeling. Mar Pet Geol, 133: 105258

Li M W, Pang X Q (2004). Contentious petroleum geochemical issues in China's sedimentary basin. Petrol Sci, 1(3): 4–22

Li Y, Chang X C, Yin W, Wang G W, Zhang J L, Shi B B, Zhang J H, Mao L X (2019). Quantitative identification of diagenetic facies and controls on reservoir quality for tight sandstones: a case study of the Triassic Chang 9 oil layer, Zhenjing area, Ordos Basin. Mar Pet Geol, 102: 680–694

Li Y, Zhang J L, Xu Y H, Chen T, Yan X, Sun L, Tian W C (2022). Genetic mechanism and grading assessment of the glutenite reservoirs in the Eocene Shahejie Formation, Chezhen Sag, Bohai Bay Basin. J Petrol Sci Eng, 211: 110226

Ma B B, Eriksson K A, Cao Y C, Jia Y C, Wang Y Z, Gill B C (2016). Fluid flow and related diagenetic processes in a rift Basin: evidence from the fourth member of the Eocene Shahejie Formation interval, Dongying Depression, Bohai Bay Basin, China. AAPG Bull, 100(11): 1633–1662

Miller K G, Kominz M A, Browning J V, Wright J D, Mountain G S, Katz M E, Sugarman P J, Cramer B S, Christie-Blick N, Pekar S F (2005). The Phanerozoic record of global sea-level change. Science, 310(5752): 1293–1298

Potter P E, Shimp N F, Witters J (1963). Trace elements in marine and fresh-water argillaceous sediments. Geochim Cosmochim Acta, 27(6): 669–694

Qian K, Shi H (1982). The choice of the method of paleosalinity determination in resource evaluation. Pet Explor Dev, 3: 32–38

Rohling E J (2007). Progress in paleosalinity: overview and presentation of a new approach. Paleoceanography, 22(3): 768–771

Schmidt G A (1999). Error analysis of paleosalinity calculation. Paleoceanography, 14(3): 422–429

Seward D (1978). Palaeosalinities and palaeotemperatures from carbon and oxygen isotopes of carbonate shells in three quaternary formations, Wanganui Basin, New Zealand. Palaeogeogr Palaeoclimatol Palaeoecol, 23: 47–55

Shi Z S, Zhu X M, Hu B, Zhang X L (2004). Sedimentary environments of Macaronichnus of the Shahejie Formation of Paleogene of Chezhen Sag in Jiyang Depression. J Paleogeography, 6(2): 207–215 (in Chinese)

Shimp N F, Witters J, Potter P E, Schleicher J A (1969). Distinguishing marine and freshwater muds. J Geol, 77(5): 566–580

Sun L, Zhang J L, Zhang T Y, Yan X, Chen T, Liu J S. (2022). Paleosalinity reconstruction for the Paleocene sequence of Lishui Sag in the East China Sea Shelf Basin. Arab J Sci Eng

Walker C T (1968). Evaluation of boron as a paleosalinity indicator and its application to offshore prospects. AAPG Bull, 52: 751–766

Walker C T, Price N B (1963). Departure curves for computing paleosalinity from boron in illites and shale. AAPG Bull, 47: 833–841

Wang Y, Guo W, Zhang G (1979). Application of some geochemical indicators in determining of sedimentary environment of the Funing group (Paleogene), Jinhu Depression, Jiangsu Province. J Tongji Univ, 2: 51–60 (in Chinese)

Wang Y, Wu P (1983). Geochemical criteria of sediments in the coastal area of Jiangsu and Zhejiang provinces. J Tongji Univ, 4: 79−87 (in Chinese)

Wei W, Algeo T J, Lu Y B, Lu Y C, Liu H, Zhang S, Peng L, Zhang J, Chen L (2018). Identifying marine incursions into the Paleogene Bohai Bay Basin lake system in northeastern China. Int J Coal Geol, 200: 1–17

Xiong X H, Xiao J F (2011). Geochemical indicators of sedimentary environments—a summary. Earth Environ, 39: 405–414 (in Chinese)

Ye C C, Yang Y B, Fang X M, Zhang W L (2016). Late Eocene clay boron-derived paleosalinity in the Qaidam Basin and its implications for regional tectonics and climate. Sediment Geol, 346: 49–59

Yuri Z N, Eder V G, Zamirailova A G (2008). Composition and formation environments of the Upper Jurassic-Lower Cretaceous black shale Bazhenov Formation (the central part of the West

Siberian Basin). Mar Pet Geol, 25(3): 289–306

Zeng L, Wang L S, Xu H X, Jiao G N, Cui S N, Han H, Zhang B S (2010). Analysis Method for Clay Minerals and Ordinary Non-clay Minerals in Sedimentary Rocks by the X-ray Diffraction. Beijing: Petroleum Industry Publishing House (in Chinese)

Zhang T F, Sun L X, Zhang Y, Cheng Y H, Li Y F, Ma H L, Lu C, Yang C, Guo G W (2016). Geochemical characteristics of the Jurassic Yan'an and Zhiluo Formations in the northern margin of Ordos Basin and their paleoenvironmental implications. Acta Geol Sin, 90: 3454–3472 (in Chinese)

Zhang X G, Lin C Y, Zahid M A, Jia X P, Zhang T (2017). Paleosalinity and water body type of Eocene Pinghu Formation, Xihu Depression, East China Sea Basin. J Petrol Sci Eng, 158: 469–478

Zheng R, Liu H (1999). Study on palaeosalinity of Chang-6 oil reservoir set in Ordos Basin. Oil Gas Geol, 20: 20–22